

Optimization of DDP test parameters through DoE for AFP process improvement

P. Dreher, A.R. Chadwick and G. Doll
DLR e.V., Institute of Structures and Design, Stuttgart, Germany

Abstract:

The optimization of the large number of parameters for the laser-assisted Automated Fiber Placement (AFP) process in order to produce high-quality laminates with high consolidation quality, low deformation and high surface quality is challenging. As a prior step towards this optimization, a closer look on how to quantify the consolidation quality in a time- and cost-effective way using the Double Drum Peel (DDP) test is given in this paper. Algorithms and methods are shown for the data processing of the test bench's output. The Design of Experiments (DoE) method is used to create experimental plans, develop surrogate models for various responses and to find optimized settings for both the peel angle and peel speed of the DDP test. The methods and results presented in this paper offer a valuable insight of how to measure the consolidation quality and how to use this information for the optimization of AFP processes.

Keywords: Automated Fiber Placement (AFP), Design of Experiments (DoE), Double Drum Peel (DDP) test

Introduction

Laser-assisted Automated Fiber Placement (AFP) process enables the time- and cost-efficient production of carbon fiber reinforced thermoplastic parts by using an industrial robot to perform the previously manual layup of material. Part consolidation can also be performed in-situ during AFP, removing the need for an oven or autoclave. An example of the AFP process is shown in Fig. 1.

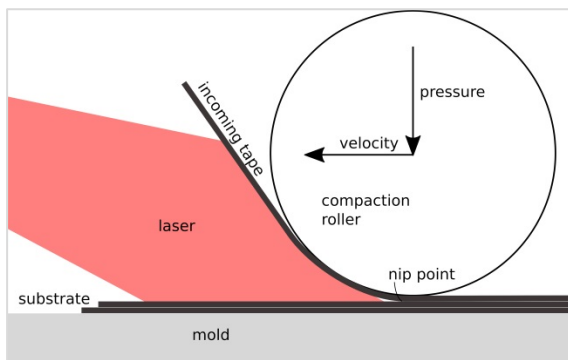


Fig. 1: AFP process

The properties of laminates produced with AFP depend on a large number of process parameters which affect the pressure, temperature and duration of the process. Examples of such process parameters are the user-defined (set) temperature at the nip point, T_{set} , the layup speed, v_{layup} , the pressure and temperature of the compaction roller, p_{roll} and T_{roll} , and the temperature of the tooling mold T_{mold} . The resultant laminate properties of major interest are the consolidation quality as well as the global deformation and part surface quality. A diagram of

the relationship between input parameters and part quality is shown in Fig. 2.

Due to the large number of input parameters, the common One-Variable-At-a-Time (OVAT) approach for process optimization is inefficient. Therefore, optimization is performed using the Design of Experiments (DoE) method. [1]

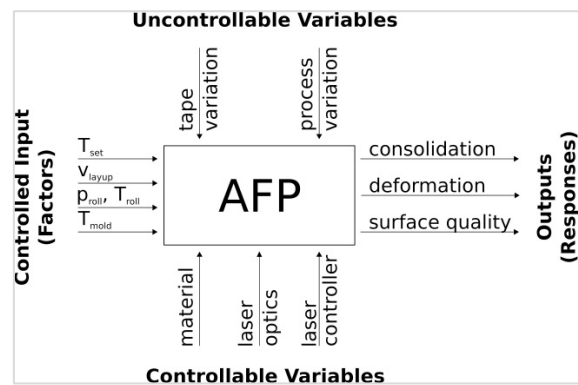


Fig. 2: Simplified black box model of the AFP process

Regardless of the method, it is essential to produce and test an adequate number of samples in order to be able to have a satisfactory approximation for the surrogate model. Measurements of specimen deformation, which are caused by thermal stresses, and of the surface quality are standardized and easy to implement. Measurements of the consolidation quality, on the other hand, are not as straightforward. The apparent inter-laminar shear strength in a three-point bending arrangement is an appropriate measure for the consolidation quality. However, the

layup and trimming of laminates to the required sample geometry and subsequent testing is time-consuming. Instead the Double Drum Peel (DDP) test, performed on the continuous peel test bench [2], is preferred. The adhesive energy of wound rings is measured by unwinding the tape through two drums while controlling the peel angle, β , drum torques, T_1 and T_2 , rotational positions, α_1 and α_2 , and the peel speed, v , as shown in Fig. 3. The peel force, F , is then computed.

The output of the DDP test is highly sensitive to β and v , with the selection of inappropriate input values causing undesired failure mechanisms to occur and hence large variance in the responses. The DoE method was chosen to iteratively narrow the design space, creating surrogate models of the responses and determining the optimized setpoint values, β_{set} and v_{set} .

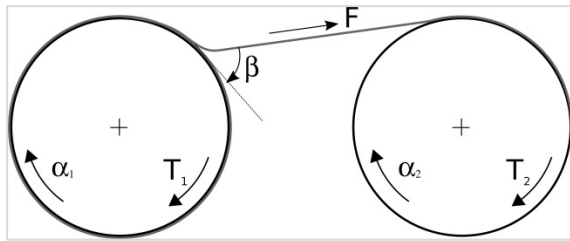


Fig. 3: Double Drum Peel (DDP) test

Materials and Methods

The total experimental plan of the DoE consisted of 35 DDP tests of rings which were wound at the tape laying facility at the DLR in Stuttgart. Every ring consisted of ten layers of CFR-PPS prepreg tape purchased from Suprem with a width of $b = 12,7$ mm.

The tests were performed in four iterations in order to augment the initial design. Since only two factors need to be optimized, a response surface design was chosen. The factors were tested in the following ranges: $13^\circ < \beta_{set} < 42^\circ$ and $50 \frac{mm}{min} < v_{set} < 350 \frac{mm}{min}$. The simplified expression for the energy release rate, G_c , with respect to the tape position, s , can be written as

$$G_c(s) = \frac{F}{b} (1 - \cos \beta) \quad (1) [3]$$

The resolution for the tape position was 0,1 mm and the error within the force measurement was less than 2 N. [2] The resultant G_c plots can be subdivided into four distinct sections:

- 1) During the transient phase, the peel arm is not yet under tension and the testing system aims to stabilize β and v . [3]

- 2) When the sealed seam is reached, the peeling force increases but is not yet sufficient for crack propagation. This region is apparent as the first climb.
- 3) A steady-state phase of length l_{set} indicates pure delamination at a constant peel force. This region is used to calculate the setpoint of the critical energy release rate, $G_{c,set}$. Local bending of the tape near the crack tip might cause fiber kinking at the pressure side of the tape as shown in Fig. 4, causing overlaying oscillations of the G_c -curve.
- 4) A second climb region follows. The increase of peel force can be explained with the occurrence of "fiber bridging", see Fig. 4.

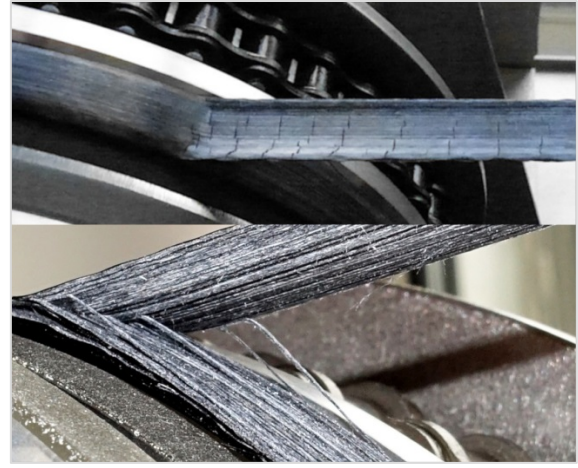


Fig. 4: Fiber kinking (top) and fiber bridging (bottom)

These regions were automatically detected by different algorithms as subsequently described. Fig. 6 displays these regions, separated with dashed vertical lines.

Different Butterworth low-pass filters were used to reduce the noise of G_c , β and v . For G_c , two different cut-off frequencies are used, resulting in $G_{c,fillt}$ and $G_{c,fillt,strong}$. The end of the transient phase was detected by analyzing the filtered signals β_{fillt} , resp. v_{fillt} and its first and second derivatives in relation to their respective median values. The tape position at which both the oscillations of β_{fillt} and v_{fillt} subsided was labelled s_{cutoff} .

Excluding all values lower than s_{cutoff} , the steady-state phase was searched between the global minimum and the following local maximum of $\frac{d^2}{ds^2} G_{c,fillt,strong}$, as shown in Fig. 5. Within this searching space, the region was detected with good agreement between G_c and its median \widetilde{G}_c . The start and end of this region, s_{start} and s_{end} , were used to calculate the length of the steady-state region.

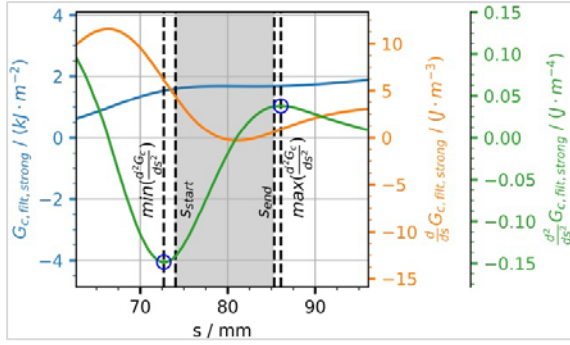


Fig. 5: Detection of the steady-state region

Within $[s_{start}, s_{end}]$, $G_{c,set}$ is calculated by taking the mean value of G_c . The standard deviations, $\sigma(G_c)$ and $\sigma(\beta)$, are then calculated as well as the deviation between $\bar{\beta}$ to its setpoint value β_{set} , $\Delta\beta$:

$$\begin{pmatrix} l_{set} \\ G_{c,set} \\ \sigma(G_c) \\ \Delta\beta \\ \sigma(\beta) \end{pmatrix} := \begin{pmatrix} s_{end} - s_{start} \\ \bar{G}_c(s) \\ \sigma(G_c(s)) \\ \bar{\beta}(s) - \beta_{set} \\ \sigma(\beta(s)) \end{pmatrix}, s_{start} \leq s \leq s_{end}$$

The amount of fiber kinking was measured in two separate ways. On the one hand, the number of breakage points within a length, $l_{amp} = 30 \text{ mm}$, was measured by manual inspection (n_{kink}). On the other hand, the number of “overshoots” n_o of $G_{c,fit}$ over $G_{c,fit,strong}$ was counted. Also, the mean value \bar{o} of all overshoots was taken. In Fig. 6, three overshoots are displayed.

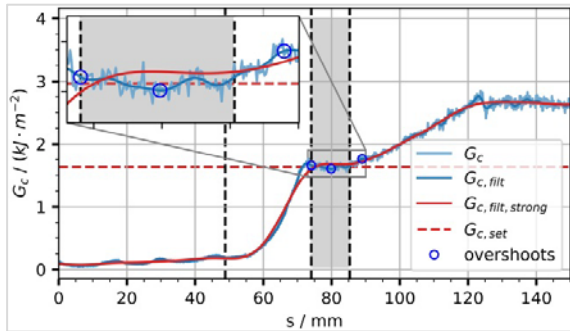


Fig. 6: Critical energy release rate G_c and overshoots

Surrogate polynomial models for the responses l_{set} , $\sigma(G_c)$, $\Delta\beta$, $\sigma(\beta)$, n_o , \bar{o} and n_{kink} were generated. ANOVA (Analysis of Variance) tables were created and analyzed for each response.

Within the optimization step, $\sigma(G_c)$, $\Delta\beta$, $\sigma(\beta)$, n_o , \bar{o} and n_{kink} were minimized whereas l_{set} was maximized. The trade-off between these objectives was done by setting limits and weighting factors.

Finally, two runs were subsequently performed near the predicted optimum for confirmation.

Results

Seven runs had to be excluded from the experimental design because the analysis routine failed to identify the distinct sections or because of large oscillations. Six of these excluded runs were located at the border of the design space and one run lacked a distinct transient phase.

ANOVA reveals that the model p-values of the surrogate models range from 0,01 to 0,15 %, implying that the model is significant. The lack-of-fit p-values range from 17 to 98 %, implying that the lack of fit is not significant relative to pure error. The surrogate models were approximated as follows:

$$\begin{pmatrix} \sigma(G_c) \\ n_{kink} \\ n_o \\ l_{set} \\ \bar{o} \\ \Delta\beta \\ \sigma(\beta) \end{pmatrix} \approx \begin{pmatrix} 99,30 & -7,73 & 2,36 & -0,60 \\ 16,97 & -2,42 & 0 & 0 \\ 8,79 & -0,62 & 0,09 & -0,04 \\ -18,15 & 1,21 & 1,13 & -0,49 \\ 164,31 & -7,14 & -3,43 & 1,47 \\ 1,05 & -0,10 & 0,09 & -0,02 \\ -0,27 & 0,01 & 0,03 & -0,01 \end{pmatrix} \begin{pmatrix} J/m^2 \\ \beta/^\circ \\ v \cdot 10^{-4} (min/m) \\ \beta v \cdot 10^{-2} (min/^\circ) \\ \beta^2 \cdot 10^{-1} (J/(^\circ m)^2) \\ v^2 \cdot 10^{-10} \left(\frac{min}{m}\right)^2 \cdot ^\circ \\ \beta^3 \cdot 10^{-3} / (^\circ)^2 \end{pmatrix} \quad (2)$$

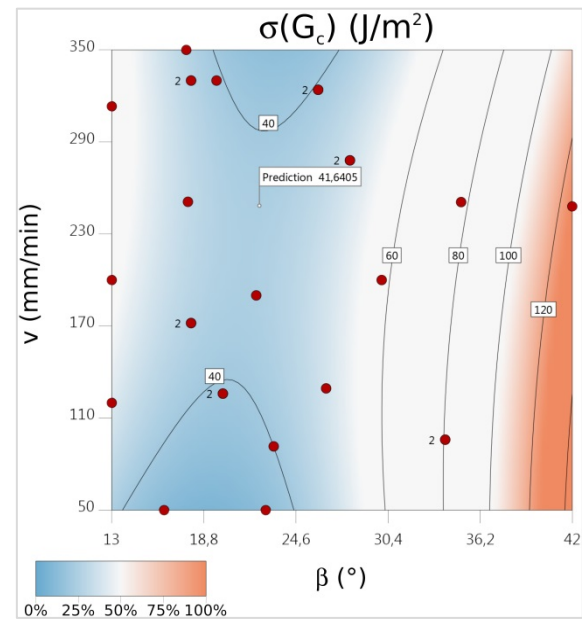


Fig. 7: Standard deviation of the critical energy release rate with design points and flagged predicted optimum

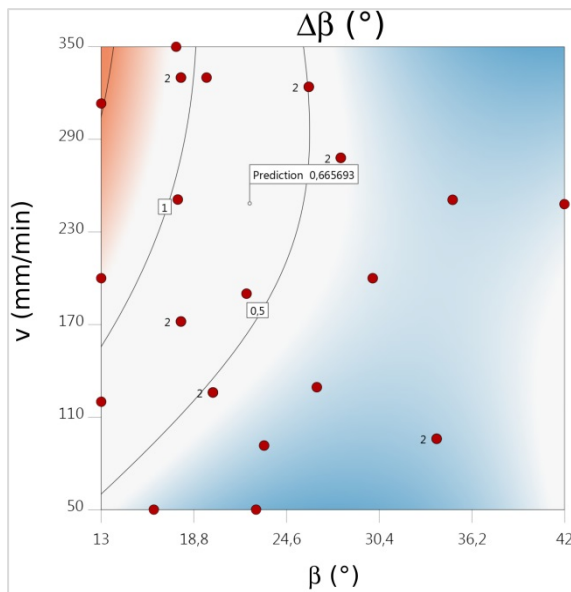


Fig. 8: Deviation of the peel angle from the setpoint value with design points and flagged predicted optimum

$s(G_c)$, n_{kink} and n_o reveal an unfavorable influence of high β -values and no significant influence of v , see exemplary Fig. 7. The remaining responses show a significant interaction effect and especially $\Delta\beta$ and $s(\beta)$ reveal undesirable results for very low values of β , see Fig. 8.

One optimum is found for $\beta \approx 22,2^\circ$ and $v \approx 248 \text{ mm/min}$. Both confirmation runs were successful: All of the measured responses were within the 95% confidence interval of the predicted values.

Discussion

The presented study reveals the importance of adequate setpoint values for β and v in order to test for pure delamination with reasonable variances and standard deviations. Sound recommendations for testing parameters of CF-PPS tape were presented which meet the recommendations stated as $20^\circ < \beta < 50^\circ$ in order to reduce energy losses due to local bending at the crack tip (fiber kinking) and to prevent both extensive tensile and bending stresses of the unattached section of the unwound ring. Furthermore, this range ensures nearly constant mode mixity of $G_{II} \approx 0,6 \cdot G_I$ between the opening mode I and the shearing mode II. [3]

n_{kink} and n_o , both quantifications for the fiber kinking effect, show similar but not identical results. Reasons for the differences are difficulties in visual inspection, since it is not obvious in all cases to distinguish between several independent kinking bands close by and one connected but discontinuous kinking band. Also, n_o is influenced by noise and the error threshold. An additional possible issue with

the data analysis might be caused by dependencies of some responses from pre-defined values such as cut-off frequencies, filter orders or threshold values.

One limitation of the DDP test is that the consolidation quality is limited to the area near the initial crack tip due to the fiber bridging effect. Another one is that testing for delamination with other layups than purely 90° layers is more complex and this might extinguish the time and cost advantage compared to other methods.

Instead of the polynomial regression within the DoE, alternative approaches such as kriging or radial basis functions might be better suited to prevent swinging up and to enable the surrogate model to develop highly nonlinear approximations, e.g. for n_{kink} and n_o which have an integer value range (step-like shape of surrogate model). Also, analyzing Pareto frontiers instead of setting weighting factors might lead to a more conclusive trade-off between the objectives.

Conclusion

The presented results are a valuable basis for a future DoE of the AFP process. The wounded rings used for quantification of the consolidation quality might also be used for quantification of the surface quality and the deformation. In case of the deformation, each ring has to be sliced and the clearance is measured, although deformation transverse to the fiber direction is not available with this method.

Acknowledgements

The presented work is part of the ICASUS project and has received funding by the European Commission through Clean Sky 2.

References

- [1] P. Schaefer, G. Gierszewski, A. Kollmannsberger, S. Zaremba and K. Drechsler, "Analysis and improved process response prediction of laser- assisted automated tape placement with PA-6/carbon tapes using DoE and numerical simulations," *Composites: Part A*, pp. 137-146, 4 November 2016.
- [2] LF Technologies, "Continuous peel test bench commercial documentation," France, 2017.
- [3] F. Daghia, C. Cluzel, L. Hébrard, F. Churlaud and B. Courtemanche, "The DDP test: a new concept to evaluate the delamination fracture toughness of cylindrical laminates," HAL, 2018.